Cortical and Trabecular Bone Healing Patterns and Quantification for Three Different Dental Implant Systems

Heloisa F. Marão, DDS, MSc, PhD[1]/Ryo Jimbo, DDS, PhD[2]/Rodrigo Neiva, DDS, MSc[3]/
Luiz Fernando Gil, DDS, MSc[4]/Michelle Bowers, DDS(c)[5]/Estevam A. Bonfante, DDS, MSc, PhD[6]/
Nick Tovar, PhD[5]/Malvin N. Janal, PhD[7]/Paulo G. Coelho, DDS, MSc, PhD[8]

Purpose: *The present study hypothesized that different bone healing patterns through initial stages of osseointegration would be observed when three distinct commercially available implant systems (Nobel Groovy, Implacil, and Zimmer TSV) were used, leading to significant variations in histometric levels of total bone and new bone formation during the osseointegration process.* ***Materials and Methods:*** *A total of 48 implants were placed bilaterally on the tibias of eight beagle dogs and allowed to heal for 2 and 6 weeks. Following euthanasia, nondecalcified specimens were processed for morphologic and histometric evaluation. Bone-to-implant contact (BIC) and new bone area fraction occupancy (BAFO) analyses for native and new bone were performed along the whole perimeter of each implant and separately for the cortical and trabecular bone regions.* ***Results:*** *Morphologic evaluation of cortical bone presented different healing patterns and osseointegration levels for different implant systems as time elapsed in vivo. Interfacial remodeling was the chief healing pattern in Zimmer implants, while a combination of interfacial remodeling and healing chambers was observed in Nobel and Implacil implants. When trabecular bone was evaluated, similar bone healing patterns were observed between systems despite different levels of osseointegration observed as a function of implantation time, implant system, and native and/or new bone BIC and BAFO.* ***Conclusion:*** *Different implant systems led to different healing patterns during early stages of osseointegration. Such variation in pattern was more noticeable in the cortical regions compared to the trabecular regions. The variation in bone healing pattern did significantly influence overall indicators of native and new BIC and BAFO during the osseointegration process. The postulated hypothesis was accepted.* Int J Oral Maxillofac Implants 2017; 32:585–592. doi: 10.11607/jomi.4856

Keywords: *bone marrow, dental implants, design, histology, osseointegration*

[1]Researcher, Department of Biomaterials and Biomimetics, New York University College of Dentistry, New York, New York, USA.
[2]Associate Professor, Department of Oral and Maxillofacial Surgery and Oral Medicine, Faculty of Odontology, Malmö University, Malmö, Sweden.
[3]Associate Professor, Department of Periodontology, University of Florida College of Dentistry, Gainesville, Florida, USA.
[4]PhD Candidate, Department of Dentistry, Division of Oral and Maxillofacial Surgery, Universidade Federal de Santa Catarina, Florianópolis, Santa Caterina, Brazil.
[5]DDS Student and Researcher, Department of Biomaterials and Biomimetics, New York University College of Dentistry, New York, New York, USA.
[6]Assistant Professor, Department of Prosthodontics, University of São Paulo, Bauru College of Dentistry, Bauru, São Paulo, Brazil.
[7]Associate Professor, Department of Epidemiology, New York University College of Dentistry, New York, New York, USA.
[8]Associate Professor, Department of Biomaterials and Biomimetics, New York University College of Dentistry, New York, New York, USA.

Correspondence to: Dr Heloisa Fonseca Marão, Rua José Padre Agostinho 1764, Curitiba, Parana, Brasil, CEP: 80710-000. Email: heloisafonsecamarao@yahoo.com.br

Dental implant treatment is highly predictable, and over the years magnitudes of in vivo studies have been conducted to further investigate the phenomenon of osseointegration.[1–3] Successful osseointegration has been proposed to be influenced by different factors, including those related to device and host.[4] While these influential factors have been widely studied, research continues to be conducted with expectations of improving bone healing through implant system design modifications.[5–12]

One of the essential but less thoroughly investigated factors in the success of osseointegration is implant macro- and microgeometry design[13–15]; for instance, it has been reported that the interaction between drilling protocols and the implant macrogeometry results in different healing patterns.[15,16] Based on the results of recent studies focusing on implant system design and drilling protocols, it can be suggested that an ideal implant system design would maintain biomechanical interlocking between the bone and the implant and, at the same time, provide a void between the osteotomy wall and the implant surface where the blood clot can be sustained and thereafter direct bone formation.[8,17]

In different healing patterns, surface engineering at both micro- and nanoscales is considered to be a viable strategy for optimizing osseointegration, since characteristics of the surface would theoretically influence the migration and attachment of growth and osteoprogenitor factors to the implant interface.[18–20] On the other hand, if the implant is placed in high-density bone and in osteotomies with a diameter similar to or smaller than the implant inner thread diameter, bone undergoes substantial cell-mediated interfacial remodeling and only after this initial remodeling process does the interaction between the osteogenic cells and the different implant surface geometries become possible. Thus, the interplay between the implant macrodesign, drilling protocols, and characteristics of the implant surface is of great importance, since the quality and quantity of osseointegration can be drastically influenced by different combinations of implant design parameters.

While a high number of studies in the literature have quantified the degree of osseointegration in terms of histomorphometry—such as bone-to-implant contact (BIC)—different healing scenarios may be occurring along the whole implant body. From both biologic and biomechanical perspectives, the influence of different healing patterns should be considered an essential factor for osseointegration since those patterns affect primary stability, the degree of interfacial remodeling that may lead to different degrees of loss of implant stability shortly after placement, and how osseointegration proceeds until achievement of secondary stability.

There is a plethora of basic osseointegration studies that conclude that implant system does affect the pattern and numeric course of histometric bone measurements until osseointegration, but a substantially smaller body of literature exists that describes and quantifies in more detail the temporal healing pattern around different implant systems placed side by side. As an example, while it is important to qualitatively describe the process of osseointegration through interfacial remodeling or healing chamber formation, biomedical engineers would also benefit from understanding how different systems' osseointegration proceeds as a function of the overall total bone and newly formed bone, as these findings may provide guidelines and insight regarding how to improve the overall bone/implant biomechanical competence as healing proceeds around implants. It would also be valuable for implant development groups to better understand how osseointegration around different implant systems proceeds as a function of bone region (ie, cortical vs trabecular), especially as bone density is variable in clinical practice.

The present study aimed to evaluate three distinct implant systems in a preclinical laboratory dog model on both cortical and trabecular bone. The present study hypothesized that different bone healing patterns through initial stages of osseointegration would be observed when three distinct commercially available implant systems (Nobel Groovy, Implacil, and Zimmer TSV) were evaluated, leading to significant variations in histometric levels of total bone and new bone formation during the osseointegration process.

MATERIALS AND METHODS

A total of 48 threaded endosseous implants (10 mm in length) with variations in bulk geometry and surface treatment were used. The implants were divided into three groups: Group A, Nobel Groovy 3.5 mm in diameter; Group B, Implacil 3.75 mm in diameter; and Group C, Zimmer TSV, 3.7 mm in diameter. The drilling technique was performed according to manufacturer recommendations.

Eight adult male beagle dogs approximately 1.5 years old were acquired after the approval of the Ethics Committee of Écólé Nationale de Vétérinaire d'Alfort, Maisons-Alfort, France. All surgical procedures were performed under general anesthesia. Medetomidine 8.5 µg/kg and morphine 0.2 mg/kg were used for premedication intravenous access. To induce general anesthesia, propofol 4 mg/kg was used. After tracheal intubation, anesthesia maintenance was performed with 2% isoflurane (adjusted for the percentage of exhaled, 1.2%) with mechanical ventilation at 10 mL/kg (approximately).

After induction of the anesthesia, both proximal tibias of each dog were shaved, prepped with an antiseptic betadine solution, and draped in the usual sterile fashion. An incision of about 5 cm was performed to access the periosteum, and a flap reflected for tibia exposure. Implants were placed on both proximal tibias in an interpolated distribution; the left and right limbs received implants at 2 and 6 weeks prior to euthanasia, respectively. Cover screws were placed to avoid tissue ingrowth. Soft tissue was sutured in layers according to standard procedures with the periosteum sutured with Vicryl 4-0 (Ethicon, Johnson & Johnson) and the skin with 4-0 Nylon (Ethicon, Johnson & Johnson).

Postoperative antibiotic and anti-inflammatory medications included a single dose of benzyl penicillin benzatine (20,000 UI/kg) intramuscularly and ketoprofen 1% (1 mL/5 kg). Euthanasia was performed by means of anesthesia overdose and the limbs were retrieved by sharp dissection. Soft tissue was removed using surgical blades, and if an implant was clinically unstable it was excluded from the study. The samples containing the implants were reduced to blocks and immersed in 10% buffered formalin solution for 24 hours. Blocks were then washed in running water for 24 hours and steadily dehydrated in a series of alcohol solutions ranging from 70% to 100% ethanol. After

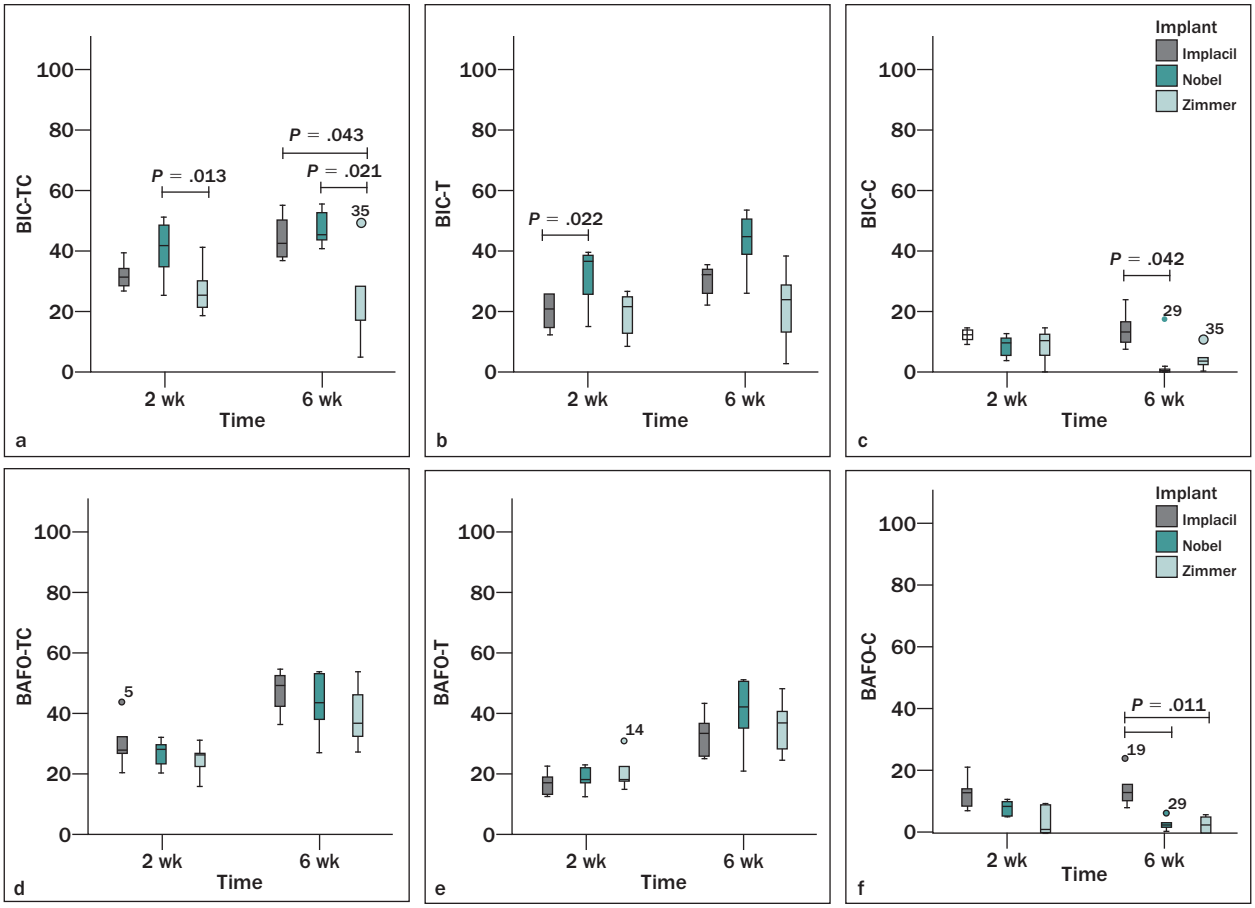

Fig 1 Box plots for total bone (native + newly formed). *(a)* Bone-to-implant contact (BIC) trabecular + cortical (BIC-TC), *(b)* BIC trabecular (BIC-T), *(c)* BIC cortical (BIC-C), *(d)* Bone area fraction occupancy (BAFO) trabecular + cortical (BAFO-TC), *(e)* BAFO trabecular (BAFO-T), *(f)* BAFO cortical (BAFO-C).

dehydration, the samples were embedded in a methacrylate-based resin (Technovit 9100, Heraeus Kulzer) according to the manufacturer's instructions. Blocks were then cut into slices (~300-µm thickness) with a precision diamond saw (Isomet 2000, Buehler), aiming the center of the implant along its long axis, and then glued to acrylic plates with an acrylate-based cement. A 24-hour setting time was allowed before grinding and polishing. Sections were then reduced to a final thickness of ~30 µm using a series of SiC abrasive papers (400, 600, 800, 1200, and 2400; Buehler) in a grinding/polishing machine (Metaserv 3000, Buehler) under water irrigation. Sections were stained with Stevenel's blue and van Gieson staining and referred to optical microscopy at ×50 to ×200 magnification (Leica DM2500M, Leica Microsystems) for histomorphologic evaluation. BIC and bone area fraction occupied (BAFO) were determined using computer software (Image J, National Institutes of Health) at ×50 to ×200 and ×100 magnification, respectively.

The regions of BIC along the implant perimeter were subtracted from the total implant perimeter, and calculations were performed to determine the BIC. The areas occupied by bone were subtracted from the total area between the threads, and calculations were performed to determine the BAFO, reported in percentages.[21] BIC and BAFO were performed for the total perimeter (along the whole implant) of the implants and separately for the cortical and trabecular bone regions. The same analyses were performed when only new bone was considered for BIC and BAFO.

Box plots were used to show the range and distribution of BIC and BAFO within each implant group as a function of time in vivo. Means were then compared by Friedman test, a distribution-free analog of the one-way repeated measures analysis of variance (ANOVA). All statistical analyses were performed with SPSS v.22 (IBM) software. Statistical significance was set to an alpha of .05.

RESULTS

Box plots representing total bone (native and newly formed bone added together) BIC and BAFO are presented in Fig 1. Figures 1a and 1d show the summary

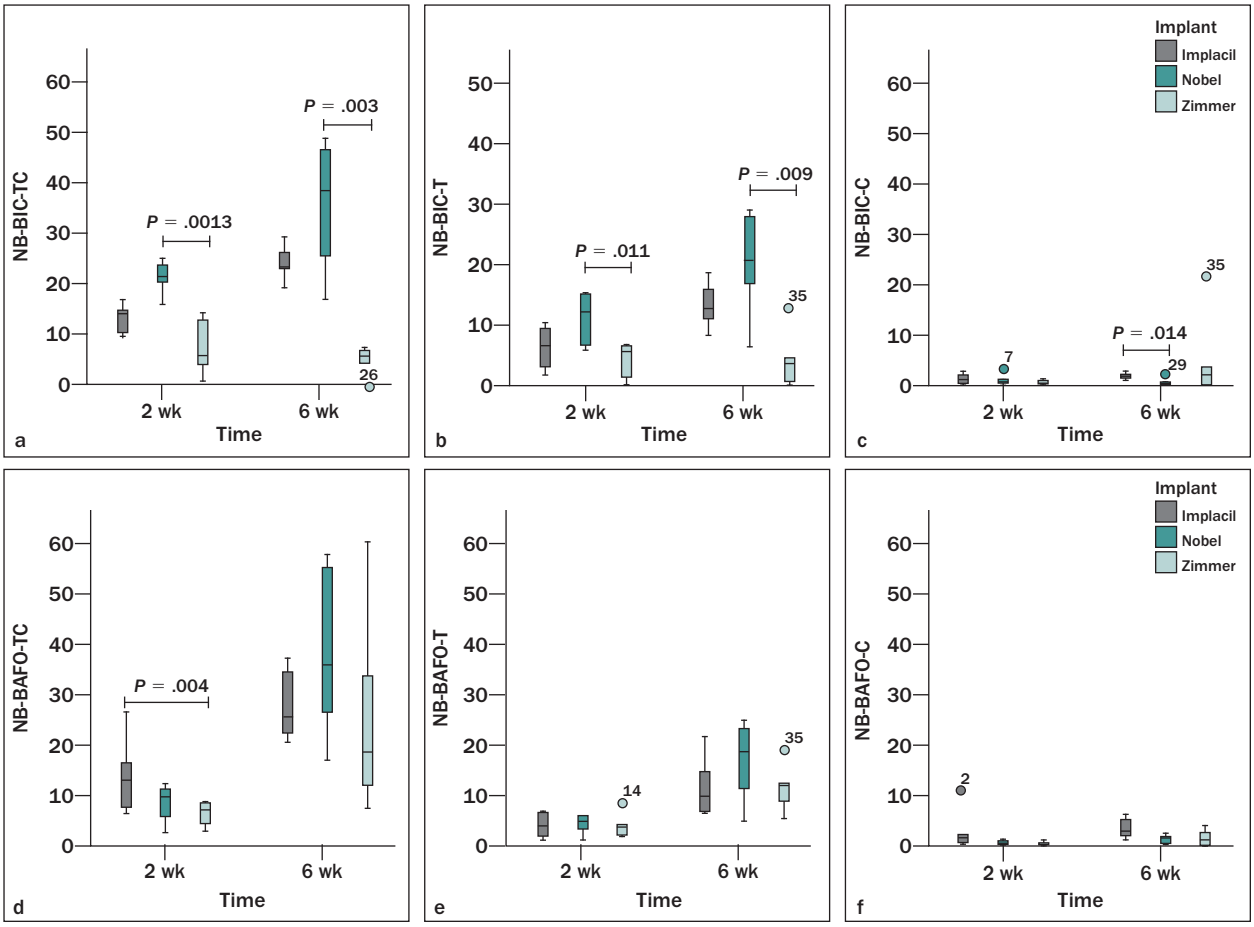

Fig 2 Box plots for new bone (NB). *(a)* Bone-to-implant contact (BIC) trabecular + cortical (NB-BIC-TC), *(b)* BIC trabecular (NB-BIC-T), *(c)* BIC cortical (NB-BIC-C), *(d)* Bone area fraction occupancy (BAFO) trabecular + cortical (NB-BAFO-TC), *(e)* BAFO trabecular (NB-BAFO-T), *(f)* BAFO cortical (NB-BAFO-C).

of total bone BIC and BAFO data for bone around the implant perimeter (trabecular + cortical, BIC-TC and BAFO-TC). Figures 1b and 1e show the BIC and BAFO data, respectively, for total bone amounts where the implant engaged the trabecular bone region (BIC-T and BAFO-T), and Figures 1c and 1f show the BIC and BAFO data, respectively, for total bone amounts where the implant engaged the cortical bone region (BIC-C and BAFO-C).

Total Bone BIC and BAFO Analysis

At 2 weeks in vivo, BIC-TC was significantly higher ($P = .013$) in the Nobel group than in the Zimmer group, and intermediate values were observed for the Implacil group. At 6 weeks, both Nobel and Implacil presented significantly higher BIC-TC ($P \leq .043$) than the Zimmer group (Fig 1a). When BIC-T at 2 weeks in vivo was considered, the highest values were observed for the Nobel group (significant compared with the Implacil group; $P = .022$). At 6 weeks in vivo, the same trend was observed but with no significant differences (Fig 1b). While no significant differences were observed between groups at 2 weeks in vivo for BIC-C, a significant difference was observed between the Implacil (highest) and Nobel (lowest) groups ($P = .042$) at 6 weeks in vivo, with Zimmer presenting intermediate values (Fig 1c). No significant differences between groups were detected when BAFO-TC (Fig 1d), BAFO-T (Fig 1e), and BAFO-C (Fig 1f) were evaluated. One exception was BAFO-C at 6 weeks; the Implacil group presented significantly higher values than the Nobel and Zimmer groups ($P = .011$) (Fig 1f).

Box plots representing the new bone BIC and BAFO relative to the total bone are presented in Fig 2 (note the different scale on the dependent variables axes relative to Fig 1 to facilitate box plot visualization). Figures 2a and 2d show the data for BIC and BAFO for new bone around the total implant perimeter (trabecular + cortical, NB-BIC-TC and NB-BAFO-TC). Figures 2b and 2e show the NB-BIC and NB-BAFO data, respectively, for new bone amounts where the implant engaged the trabecular bone region (NB-BIC-T and NB-BAFO-T), and Figures 2c and 2f show the NB-BIC and NB-BAFO data, respectively, for new bone amounts where the

implant engaged the cortical bone region (NB-BIC-C and NB-BAFO-C).

New Bone BIC and BAFO Analysis

At both 2 and 6 weeks, NB-BIC-TC (Fig 2a) and NB-BIC-T (Fig 2b) presented identical patterns, with the Nobel group presenting significantly higher values than the Zimmer group ($P \leq .013$) and the Implacil group presenting intermediate levels. No significant differences between groups were detected for the NB-BIC at 2 weeks in vivo, while at 6 weeks in vivo a significant difference ($P = .014$) was observed between the Implacil (highest) and Nobel (lowest) groups with the Zimmer group presenting intermediate values (Fig 2c). No significant differences between groups were detected when NB-BAFO-TC (Fig 2d), BAFO-T (Fig 2e), and BAFO-C (Fig 2f) were evaluated. One exception was NB-BAFO-TC at 2 weeks; the Implacil group presented significantly higher values than the Zimmer group ($P = .011$) with the Nobel group presenting intermediate values (Fig 2f).

Morphologic evaluation of the histologic slides depicted direct bone contact to the implant surface and the proximity to both cortical and trabecular regions at both time points evaluated. An overall qualitative increase in bone around the implant was also observed for all groups from 2 to 6 weeks in vivo.

Morphologic Description of Cortical Bone Healing

When the interaction between implant and cortical bone was evaluated, significantly different healing patterns occurred among groups (Fig 3). At 2 weeks in vivo, the Nobel group presented a looser relationship between its surgical instrumentation and the implant inner diameter, which resulted in formation of healing chambers at the cortical region (Fig 3a). No microcracking or bone remodeling were observed where the implant threads engaged cortical bone. A similar relationship between surgical instrumentation and implant inner diameter was observed for the Implacil group at the cortical region (Fig 3b), although these formed smaller healing chambers than the Nobel group (Fig 3a). In the Implacil group, bone microcracking along with interfacial remodeling was observed where implant threads engaged cortical bone (Fig 3b). Both the Nobel and Implacil groups' histologic sections depicted the surgical instrumentation line outer diameter in native bone presenting as the healing chamber outer boundary (considering the inner diameter of the implant as the inner boundary) (Figs 3a and 3b). The larger healing chambers observed for the Nobel group were filled with stroma, and the smaller healing chambers formed around Implacil implants were filled with stroma along with initial woven bone formation. A different initial interaction between implant and bone was observed for the Zimmer group (Fig 3c), in which substantial interfacial remodeling was taking place at the cortical bone-implant interface. In this group, no obvious instrumentation line was present and a gap between implant and cortical bone was evident due to interfacial remodeling (Fig 3c).

From 2 to 6 weeks, different healing characteristics were observed between groups (Fig 3). For the Nobel group, a retraction of the instrumentation outer diameter line was observed, resulting in larger healing chambers, at this time partially filled with woven bone (Fig 3d). Interfacial remodeling sites were observed in regions where direct engagement with the implant crest module/implant threads and cortical bone existed immediately after implantation and led to a gap

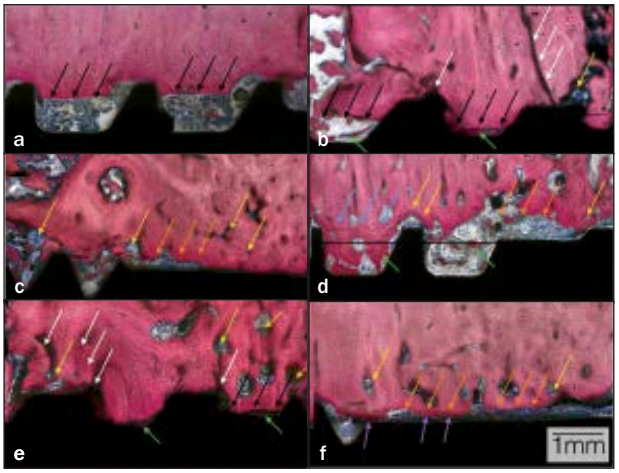

Fig 3 Stevenel's blue and van Gieson stained optical micrographs of implant group healing chambers in the cortical bone. *(a)* Nobel, *(b)* Implacil, and *(c)* Zimmer at 2 weeks. *(d)* Nobel, *(e)* Implacil, and *(f)* Zimmer at 6 weeks. At 2 weeks in vivo, the *(a)* Nobel and *(b)* Implacil bone-implant interfaces presented the surgical instrumentation line outer diameter (black arrows) bounding healing chambers along with the implant threads and inner diameter. These healing chambers were filled with stroma and woven bone (green arrows). Microcracks (white arrows) and active remodeling sites around the implants (yellow arrow) were observed for different groups at this time in vivo. A gap between the implant and cortical bone (orange arrows) and the interfacial active remodeling site (yellow arrows) was observed for the *(c)* Zimmer group at 2 weeks. At 6 weeks, the *(d)* Nobel group bone-implant interface presented a retraction of the instrumentation outer diameter line (from the solid black line to the area denoted by the blue arrows), filled with woven bone (green arrows). Note the extensive gap between implant and cortical bone (orange arrows) and the interfacial remodeling sites (yellow arrows). For the *(e)* Implacil group at 6 weeks, the microcracks (white arrows) were undergoing remodeling along with more intense levels of interfacial remodeling (yellow arrows). The black arrows depict the surgical instrumentation line and healing chambers filled with woven bone (green arrows). For the *(f)* Zimmer group at 6 weeks, the gap (orange arrows) between implant and cortical bone due to the interfacial remodeling (yellow arrows) was still detected and initial bone formation from the native remodeled bone toward the implant surface (purple arrows) was observed.

Fig 4 Stevenel's blue and van Gieson stained low magnification optical micrographs of implant groups in the trabecular bone. *(a)* Nobel, *(b)* Implacil, and *(c)* Zimmer at 2 weeks. *(d)* Nobel, *(e)* Implacil, and *(f)* Zimmer at 6 weeks.

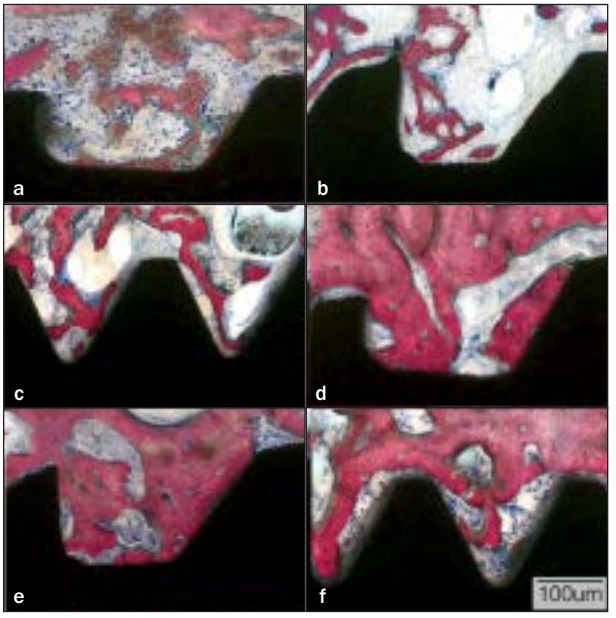

Fig 5 Higher magnification of the different implant groups at the trabecular region of interest. *(a)* Nobel, *(b)* Implacil, and *(c)* Zimmer at 2 weeks. *(d)* Nobel, *(e)* Implacil, and *(f)* Zimmer at 6 weeks. At 2 weeks, initial bone formation at the implant surface was more intense for the *(a)* Nobel group relative to the other two groups. At 6 weeks (d, e, f), higher degrees of bone in direct contact and in proximity with all implant surfaces were observed.

between implant and cortical bone along the implant perimeter (Fig 3d). The interfacial remodeling between cortical bone and Implacil implants was observed to be occurring at regions of microcracks, along with the interfacial remodeling occurring where the implant engaged cortical bone after placement (Fig 3e). Woven bone was observed in the small healing chambers formed due to the mismatch between final drill diameter and implant inner diameter (Fig 3e). Substantial interfacial remodeling between cortical bone and the Zimmer implant crest module was also observed (Fig 3f), and initial bone formation from the native bone toward (bone reverse line) the implant surface was observed.

Morphologic Description of Trabecular Bone Healing

Figure 4 represents the trabecular bone region of interest of all groups at 2 and 6 weeks and depicts the notable increase in bone in proximity with the implant surface from 2 to 6 weeks, demonstrating the osseoconductive and biocompatible properties of each implant surface. Higher magnification (Fig 5) of bone-implant interfaces of the different groups at the trabecular bone region of interest showed that contact osteogenesis occurred in all implant groups. At 2 weeks, initial bone formation at the implant surface was more pronounced in the Nobel group (Fig 5a) than in the other two groups, which was represented by lower degrees of bone formation in direct contact with the implant surface in the Implacil and Zimmer groups (Figs 5b and 5c). Bone formation in proximity to the implant surface was observed in all groups. At 6 weeks, higher degrees of bone in direct contact and in proximity to the implant surfaces were observed (Figs 5d–5f).

DISCUSSION

Literature has suggested that metallic bioinert/biocompatible devices are capable of osseointegration and insignificant differences can be observed in clinical performances with a 5-year success rate of around 90% to 95%.[22] The textured surface that is applied to most commercially available dental implant systems has contributed to the success of those dental implant systems, especially in areas of reduced bone quality.[23–25] The surfaces of the implants tested in the current study have unique characteristics with sufficient documentation. The surface on the Nobel Groovy implants (TiUnite) is generated through anodic oxidation, in which a thick amorphous oxide layer of approximately 10 µm is formed on the implant surface.[26] The surface of the Zimmer TSV implants possesses a microtextured surface generated by hydroxyapatite particle blasting.[27] This microtextured surface possesses numerous micropits on the surface owing to the

blasting procedure. The Implacil implants also possess a microtextured surface made through a titanium oxide particle grit blasting/acid-etching protocol.[6] These features have been suggested to be advantageous for rapid bone apposition to the implant.

However, it is also a fact that machined implant surfaces osseointegrate and clinically function in a manner comparable to that of these surfaces.[22,28,29] This is an indication that for successful achievement and maintenance of osseointegration, factors other than implant surface also play an important role. For instance, Gil et al[30] reported the outcomes up to 18 years of clinically functional implants. In this histologic observation, it was suggested that the line where the osteotomy was initially created was still distinguishable after many years in function, suggesting the importance of initial drilling procedures and their interactions with the implant macrogeometry. Based on these findings, Coelho et al[17] have emphasized the importance of different healing modes generated by the implant hardware design; moreover, it was suggested that the modifications at the micro- and nanolevels of the recent commercially available implants have the potential to further exert their osteogenic properties if the implant hardware design was optimized.

The present study investigated whether three different commercially available implant systems with different macrogeometries and different drilling protocols would influence healing kinetics to achieve osseointegration. The macrogeometry of each implant system was distinct, as was evident from the histologic micrographs. The Nobel and Implacil implants possessed a buttress thread design, and the Zimmer surface possessed a v-threaded design.[31]

The histologic and histomorphometric results showed that distinct healing kinetics were observed among the three study groups owing to the interplay between the drilling protocols and the respective macrogeometries. Of interest was that the Nobel group presented the highest BIC values for both 2 and 6 weeks. This is an indication that the interplay between the macrogeometry (which generated a healing chamber) and the implant surface topography most stimulated bone apposition to the implant surface. The chamber or void generated has been reported to sustain blood clots,[16,32] which are rich in osteoblast precursors and growth factors.[33,34]

The BAFO value was of some interest, showing that there was a trend for the Implacil group to possess higher percentages of BAFO. This phenomenon could be the result of the interplay between the drill protocol and the macrogeometry, in that the degree of implant thread interlocking the surrounding bone could determine the amount of bone fill within the threads. Although the bone initially in contact with the implant will undergo bone resorption due to surgical trauma and osteocompression necrosis, reportedly of up to 500 µm,[35] the initial bone in contact is important for the mechanical stability of the implant until osseointegration takes place.[36,37]

Thus, from the outcomes obtained, it can be suggested that the differences in osseointegration properties observed within the healing chambers were influenced by the distinct surface characteristics of the different implant systems, surgical instrumentation, and implant macrogeometry. Thus, understanding the bone healing processes of these systems may provide indications as to when the implant can be functionally loaded. However, it must be noted here that the short observation period is the most significant limitation of the current study and longer observations are necessary to better characterize the osseointegration properties of the different systems. Such limitations should be considered in future studies to observe the effect of implant hardware design and drilling protocols.

CONCLUSIONS

The present study hypothesized that different cortical and trabecular bone healing patterns through initial stages of osseointegration would be observed when three distinct commercially available implant systems (Nobel Groovy, Implacil, and Zimmer TSV) were evaluated, leading to significant variations in histometric levels of total bone and new bone formation during the osseointegration process. These results showed that the interplay between implant design and drilling sequences had an influence on the temporal events leading to successful osseointegration through interfacial remodeling, healing chamber formation, or a combination of both. From a numeric histometric standpoint, the implant systems tested did significantly influence osseointegration indicator markers BIC and BAFO during the osseointegration process. Altogether, the results obtained in the present study validated the hypothesis.

ACKNOWLEDGMENTS

This study was funded by Implacil. The authors declare no conflicts of interest related to this study.

REFERENCES

1. Albrektsson T, Sennerby L. Direct bone anchorage of oral implants: Clinical and experimental considerations of the concept of osseointegration. Int J Prosthodont 1990;3:30–41.
2. Albrektsson T, Jacobsson M. Bone-metal interface in osseointegration. J Prosthet Dent 1987;57:597–607.

3. Scipioni A, Bruschi GB, Giargia M, Berglundh T, Lindhe J. Healing at implants with and without primary bone contact. An experimental study in dogs. Clin Oral Implants Res 1997;8:39–47.
4. Albrektsson T, Branemark PI, Hansson HA, Lindström J. Osseointegrated titanium implants. Requirements for ensuring a long-lasting, direct bone-to-implant anchorage in man. Acta Orthop Scand 1981;52:155–170.
5. Elias CN, Rocha FA, Nascimento AL, Coelho PG. Influence of implant shape, surface morphology, surgical technique and bone quality on the primary stability of dental implants. J Mech Behav Biomed Mater 2012;16:169–180.
6. Jimbo R, Tovar N, Anchieta RB, et al. The combined effects of undersized drilling and implant macrogeometry on bone healing around dental implants: An experimental study. Int J Oral Maxillofac Surg 2014;43:1269–1275.
7. Dos Santos MV, Elias CN, Cavalcanti Lima JH. The effects of superficial roughness and design on the primary stability of dental implants. Clin Implant Dent Relat Res 2011;13:215–223.
8. Jimbo R, Janal MN, Marin C, Giro G, Tovar N, Coelho PG. The effect of implant diameter on osseointegration utilizing simplified drilling protocols. Clin Oral Implants Res 2014;25:1295–1300.
9. Coelho PG, Bonfante EA, Pessoa RS, et al. Characterization of five different implant surfaces and their effect on osseointegration: A study in dogs. J Periodontol 2011;82:742–750.
10. Coelho PG, Takayama T, Yoo D, et al. Nanometer-scale features on micrometer-scale surface texturing: A bone histological, gene expression, and nanomechanical study. Bone 2014;65:25–32.
11. Teixeira HS, Marin C, Witek L, et al. Assessment of a chair-side argon-based non-thermal plasma treatment on the surface characteristics and integration of dental implants with textured surfaces. J Mech Behav Biomed Mater 2012;9:45–49.
12. Shibli JA, Grassi S, Piattelli A, et al. Histomorphometric evaluation of bioceramic molecular impregnated and dual acid-etched implant surfaces in the human posterior maxilla. Clin Implant Dent Relat Res 2010;12:281–288.
13. Bonfante EA, Granato R, Marin C, et al. Early bone healing and biomechanical fixation of dual acid-etched and as-machined implants with healing chambers: An experimental study in dogs. Int J Oral Maxillofac Implants 2011;26:75–82.
14. Marin C, Granato R, Suzuki M, et al. Biomechanical and histomorphometric analysis of etched and non-etched resorbable blasting media processed implant surfaces: An experimental study in dogs. J Mech Behav Biomed Mater 2010;3:382–391.
15. Coelho PG, Suzuki M, Guimaraes MV, et al. Early bone healing around different implant bulk designs and surgical techniques: A study in dogs. Clin Implant Dent Relat Res 2010;12:202–208.
16. Berglundh T, Abrahamsson I, Lang NP, Lindhe J. De novo alveolar bone formation adjacent to endosseous implants. Clin Oral Implants Res 2003;14:251–262.
17. Coelho PG, Jimbo R, Tovar N, Bonfante EA. Osseointegration: Hierarchical designing encompassing the macrometer, micrometer, and nanometer length scales. Dent Mater 2015;31:37–52.
18. Guastaldi FP, Yoo D, Marin C, et al. Plasma treatment maintains surface energy of the implant surface and enhances osseointegration. Int J Biomater 2013;2013:354125.
19. Biggs MJ, Richards RG, Gadegaard N, et al. Interactions with nanoscale topography: Adhesion quantification and signal transduction in cells of osteogenic and multipotent lineage. J Biomed Mater Res A 2009;91:195–208.
20. Coelho PG, Granjeiro JM, Romanos GE, et al. Basic research methods and current trends of dental implant surfaces. J Biomed Mater Res B Appl Biomater 2009;88:579–596.
21. Leonard G, Coelho P, Polyzois I, Stassen L, Claffey N. A study of the bone healing kinetics of plateau versus screw root design titanium dental implants. Clin Oral Implants Res 2009;20:232–239.
22. Jimbo R, Albrektsson T. Long-term clinical success of minimally and moderately rough oral implants: A review of 71 studies with 5 years or more of follow-up. Implant Dent 2015;24:62–69.
23. Khang W, Feldman S, Hawley CE, Gunsolley J. A multi-center study comparing dual acid-etched and machined-surfaced implants in various bone qualities. J Periodontol 2001;72:1384–1390.
24. Stach RM, Kohles SS. A meta-analysis examining the clinical survivability of machined-surfaced and osseotite implants in poor-quality bone. Implant Dent 2003;12:87–96.
25. Pinholt EM. Brånemark and ITI dental implants in the human bone-grafted maxilla: A comparative evaluation. Clin Oral Implants Res 2003;14:584–592.
26. Sawase T, Jimbo R, Wennerberg A, Suketa N, Tanaka Y, Atsuta M. A novel characteristic of porous titanium oxide implants. Clin Oral Implants Res 2007;18:680–685.
27. Mazor Z, Cohen DK. Preliminary 3-dimensional surface texture measurement and early loading results with a microtextured implant surface. Int J Oral Maxillofac Implants 2003;18:729–738.
28. Simion M, Benigni M, Al-Hezaimi K, Kim D. Early bone formation adjacent to oxidized and machined implant surfaces: A histologic study. Int J Periodontics Restorative Dent 2015;35:9–17.
29. Simion M, Gionso L, Grossi GB, Briguglio F, Fontana F. Twelve-year retrospective follow-up of machined implants in the posterior maxilla: Radiographic and peri-implant outcome. Clin Implant Dent Relat Res 2015;17(suppl 2):e343–e351.
30. Gil LF, Suzuki M, Janal MN, et al. Progressive plateau root form dental implant osseointegration: A human retrieval study. J Biomed Mater Res B Appl Biomater 2015;103:1328–1332.
31. Chowdhary R, Halldin A, Jimbo R, Wennerberg A. Evaluation of stress pattern generated through various thread designs of dental implants loaded in a condition of immediately after placement and on osseointegration—An FEA study. Implant Dent 2013;22:91–96.
32. Meirelles L, Brånemark PI, Albrektsson T, Feng C, Johansson C. Histological evaluation of bone formation adjacent to dental implants with a novel apical chamber design: Preliminary data in the rabbit model. Clin Implant Dent Relat Res 2015;17:453–460.
33. Geiger F, Bertram H, Berger I, et al. Vascular endothelial growth factor gene-activated matrix (VEGF165-GAM) enhances osteogenesis and angiogenesis in large segmental bone defects. J Bone Miner Res 2005;20:2028–2035.
34. Maes C, Kobayashi T, Selig MK, et al. Osteoblast precursors, but not mature osteoblasts, move into developing and fractured bones along with invading blood vessels. Dev Cell 2010;19:329–344.
35. Eriksson RA, Albrektsson T, Magnusson B. Assessment of bone viability after heat trauma: A histological, histochemical and vital microscopic study in the rabbit. Scand J Plast Reconstr Surg 1984;18:261–268.
36. Coelho PG, Jimbo R. Osseointegration of metallic devices: Current trends based on implant hardware design. Arch Biochem Biophys 2014;561:99–108.
37. Halldin A, Jimbo R, Johansson CB, et al. The effect of static bone strain on implant stability and bone remodeling. Bone 2011;49:783–789.